Fusogenic micropeptide Myomixer is essential for satellite cell fusion and muscle regeneration

Pengpeng Bi[a,b,c], John R. McAnally[a,b,c], John M. Shelton[d], Efrain Sánchez-Ortiz[a,b,c], Rhonda Bassel-Duby[a,b,c], and Eric N. Olson[a,b,c,1]

[a]Department of Molecular Biology, University of Texas Southwestern Medical Center, Dallas, TX 75390; [b]Hamon Center for Regenerative Science and Medicine, University of Texas Southwestern Medical Center, Dallas, TX 75390; [c]Senator Paul D. Wellstone Muscular Dystrophy Cooperative Research Center, University of Texas Southwestern Medical Center, Dallas, TX 75390; and [d]Department of Internal Medicine, University of Texas Southwestern Medical Center, Dallas, TX 75390

Contributed by Eric N. Olson, March 1, 2018 (sent for review January 3, 2018; reviewed by Bradley B. Olwin and Nadia A. Rosenthal)

Regeneration of skeletal muscle in response to injury occurs through fusion of a population of stem cells, known as satellite cells, with injured myofibers. Myomixer, a muscle-specific membrane micropeptide, cooperates with the transmembrane protein Myomaker to regulate embryonic myoblast fusion and muscle formation. To investigate the role of Myomixer in muscle regeneration, we used CRISPR/Cas9-mediated genome editing to generate conditional knockout Myomixer alleles in mice. We show that genetic deletion of Myomixer in satellite cells using a tamoxifen-regulated Cre recombinase transgene under control of the Pax7 promoter abolishes satellite cell fusion and prevents muscle regeneration, resulting in severe muscle degeneration after injury. Satellite cells devoid of Myomixer maintain expression of Myomaker, demonstrating that Myomaker alone is insufficient to drive myoblast fusion. These findings, together with prior studies demonstrating the essentiality of Myomaker for muscle regeneration, highlight the obligatory partnership of Myomixer and Myomaker for myofiber formation throughout embryogenesis and adulthood.

skeletal muscle | fusion | satellite cells | Myomaker | CRISPR/Cas9

Skeletal muscle is the largest tissue in the body, accounting for ~40% of human body mass. Skeletal muscle formation involves the differentiation and fusion of myoblasts to form multinucleated myofibers (1, 2). In adult skeletal muscle, resident muscle stem cells, called satellite cells (SCs), are required for muscle growth, maintenance, and regeneration (3–5). SCs are characterized by their unique anatomical location between the basal lamina and plasma membrane of myofibers (6). Under normal conditions, SCs are quiescent, whereas in response to injury they become activated and enter the cell cycle before their terminal differentiation and fusion into myofibers (7, 8). SCs are marked by the expression of the paired-box transcription factor, Pax7, and deletion of Pax7 from SCs prevents muscle regeneration (9).

The formation of myofibers through cell–cell fusion involves a series of events, including cell–cell recognition and adhesion, cytoskeletal reorganization, and, ultimately, membrane merger (10). Although a variety of proteins have been shown to participate in myoblast fusion (11, 12), much remains to be learned about the underlying mechanisms and the interplay between muscle-specific and ubiquitous components of the fusion process. Recently, we discovered two muscle-specific membrane proteins, Myomaker and Myomixer, which are essential for myoblast fusion during embryogenesis (13, 14). Myomaker is a seven-pass transmembrane protein capable of promoting fusion of fibroblasts with myoblasts (13, 15). Myomixer, also referred to as Myomerger (16) and Minion (17), is a micropeptide which lacks autonomous fusogenic activity, but stimulates the fusogenic activity of Myomaker (14, 16, 17). Moreover, coexpression of this pair of membrane proteins is sufficient to confer fusogenic potential to cell types that otherwise cannot fuse (14, 16, 17). Genetic deletion of Myomaker or Myomixer abolishes myoblast fusion and muscle formation during embryogenesis in mice and zebrafish (14, 16–20). Myomaker is also required for fusion of SCs during adult muscle regeneration (21).

Myomaker and Myomixer are up-regulated in SCs during muscle regeneration (14, 16, 17, 21). However, the perinatal lethality of Myomixer null mice has precluded an analysis of its potential involvement in myofiber regeneration in response to injury (14). To directly assess the potential involvement of Myomixer in SC-mediated muscle regeneration, we generated mice with conditional *Myomixer* null alleles, which were deleted in SCs of adult mice with a tamoxifen (TMX)-inducible Cre recombinase controlled by the Pax7 promoter (22). We show that Myomixer is essential for the fusion of regenerative SCs and the formation of new myofibers after injury of adult muscle. The absence of Myomixer in SCs results in dramatic muscle degeneration following injury, despite the expression of Myomaker in these cells. Thus, at every stage of vertebrate myogenesis examined thus far, Myomixer and Myomaker function in an obligatory partnership to control myoblast fusion and myofiber formation.

Results

Conditional Deletion of Myomixer in Mice. Germline *Myomixer* null mice display perinatal lethality due to an absence of multinucleated myofibers (14), precluding an analysis of Myomixer function in adulthood. To circumvent the lethality of *Myomixer* null mice, we generated mice with conditional null alleles of the

Significance

Skeletal muscle damaged by injury or disease can regenerate new muscle fibers. The regenerative properties of skeletal muscle involve fusion of activated muscle stem cells (satellite cells). We recently discovered Myomixer, a conserved micropeptide that is specifically expressed during muscle formation. Myomixer, together with its partner Myomaker, another muscle-specific membrane protein, is necessary for muscle formation during embryogenesis. Here, we show the absolute requirement of Myomixer for the fusion of satellite cells and regeneration of adult muscle in response to injury. Our findings provide insights into the mechanisms of muscle formation and suggest opportunities for enhancing muscle regeneration through manipulation of Myomixer and Myomaker.

Author contributions: P.B., R.B.-D., and E.N.O. designed research; P.B., J.R.M., J.M.S., and E.S.-O. performed research; P.B., J.R.M., J.M.S., E.S.-O., and E.N.O. analyzed data; and P.B., R.B.-D., and E.N.O. wrote the paper.

Reviewers: B.B.O., University of Colorado; and N.A.R., The Jackson Laboratory.

The authors declare no conflict of interest.

[1]To whom correspondence should be addressed. Email: Eric.Olson@utsouthwestern.edu.

This article contains supporting information online at www.pnas.org/lookup/suppl/doi:10.1073/pnas.1800052115/-/DCSupplemental.

Published online March 26, 2018.

Myomixer gene using clustered regularly interspaced short palindromic repeats (CRISPR) and Cas9 endonuclease-mediated homology-directed repair (HDR) to insert loxP sites flanking *Myomixer* exons. Of note, the *Myomixer* gene encodes two isoforms: a short isoform of 84 amino acids translated from an ORF in exon 3, and a longer isoform of 108 amino acids translated from an extended ORF in exons 2 and 3. Through examination of RNA-seq data of C2C12 myoblasts (23), we found that the short isoform is the predominantly expressed isoform during myoblast differentiation (Fig. S1*A*). Nevertheless, to discern any potential function of the 24-amino acid N-terminal region of the long isoform of Myomixer, we generated two floxed *Myomixer* alleles, termed *Mymx*^{loxP1,2} and *Mymx*^{loxP3,4}, allowing deletion of the short and long isoforms by inserting two loxP sites flanking exon 3 (Fig. 1*A*) or exons 1–3 (Fig. 1*E*), respectively.

Mouse zygotes were injected with five components for each targeting scheme: two single guide RNAs (sgRNAs) targeted to sequences flanking *Myomixer* exons; two single-stranded oligodeoxynucleotide DNA (ssODNA) donors, each containing a loxP site flanked by short arms with homology to the desired insertion site; and Cas9 mRNA (Fig. 1 *A* and *E*). Cas9 nuclease asymmetrically releases the cleaved DNA strand that is not complementary to the sgRNA (the nontarget strand) (24). As such, improved HDR efficiency was reported in the presence of an asymmetric target-strand donor ssODNA overlapping the Cas9 cut site with 36 base pairs (bp) on the protospacer-adjacent motif (PAM)-distal side, and a 91-bp extension on the PAM-proximal side of the cleavage (24). The ssODNAs of this design were named ssODNA1–4, allowing HDR-mediated insertion of loxP sites 1–4 after cutting by sgRNA1–4 (Fig. 1 *A* and *E*).

Genotyping of filial 0 (F0) *Mymx*^{loxP1,2} mice with two pairs of primers flanking loxP1 (Fig. 1*B*) or loxP2 sites (Fig. 1*C*) and another pair of primers flanking both loxP sites revealed 10% (2 out of 20 mice) correct targeting efficiency, although large deletions and the insertion of a single loxP site were also observed. We confirmed the simultaneous insertions of the loxP1 and loxP2 sites from two founder F0 mice after cloning and sequencing a mixture of PCR products (Fig. S1 *B* and *C*). In parallel, a targeting efficiency of 14% (4 out of 28 mice) was achieved for the generation of F0 *Mymx*^{loxP3,4} mice. The simultaneous insertions of the loxP3 (Fig. 1*F*) and loxP4 (Fig. 1*G*) sites from these founders were also confirmed by cloning and sequencing of genomic PCR products (Fig. S1 *E* and *F*).

We isolated intramuscular fibroblasts from F1 *Mymx*$^{loxP1,2/+}$ and *Mymx*$^{loxP3,4/+}$ mice to validate the functionality of the loxP sites in allowing Cre-mediated DNA recombination of the Myomixer ORFs. Primary fibroblasts were infected with recombinant adenoviruses expressing GFP or Cre recombinase. Forty-eight hours postviral infection, genomic DNA was extracted from these cells and subjected to PCR amplification and sequence analysis with a

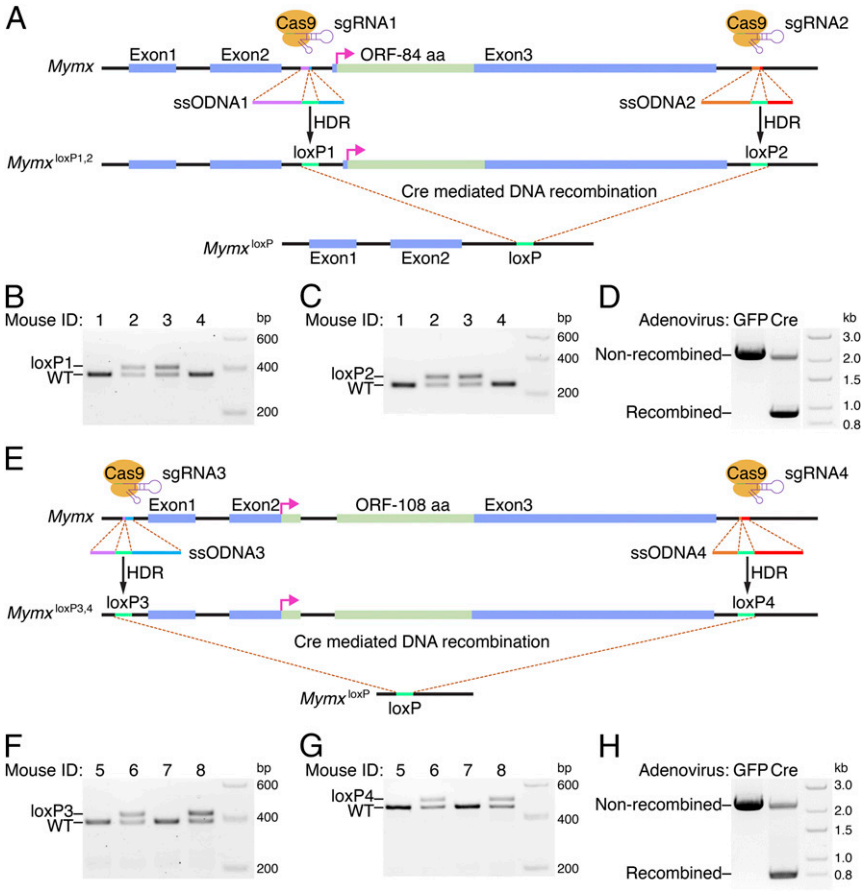

Fig. 1. Generation of *Myomixer*^{loxP} alleles. (*A*) Schematic of experimental design to insert loxP1 and loxP2 sites into intron 2 and the 3′-UTR region of the *Myomixer* (*Mymx*) gene, respectively. Note that upon Cre-mediated DNA recombination, the short Myomixer isoform is removed. (*B* and *C*) PCR genotyping with primers that amplify the regions where the loxP1 and loxP2 sites were inserted. (*D*) PCR amplification of genomic DNA isolated from *Mymx*$^{loxp1,2/+}$ fibroblasts at 48 h postadenoviral infection. (*E*) Schematic of experimental design to insert loxP3 and loxP4 sites into the 5′- and 3′-UTR regions of the *Myomixer* gene, respectively. Note that upon Cre-mediated DNA recombination, the ORF encoding the long Myomixer isoform is removed. (*F* and *G*) PCR genotyping with primers that amplify the regions where the loxP3 and loxP4 sites were inserted. (*H*) PCR amplification of genomic DNA isolated from *Mymx*$^{loxp3,4/+}$ fibroblasts at 48 h postadenoviral infection. ssODNA, single-stranded oligodeoxynucleotide DNA. HDR, homology-directed repair.

pair of primers flanking these loxP sites. Gel electrophoresis of the PCR products showed DNA bands of expected sizes in the absence and presence of genomic recombination in both *Mymx*$^{loxP1,2/+}$ and *Mymx*$^{loxP3,4/+}$ loci (Fig. 1 *D* and *H*). We confirmed the correct DNA recombination in fibroblasts isolated from all these lines of *Mymx*^{loxP} mice by cloning and sequencing PCR products (Fig. S1 *D* and *G*).

Deletion of Myomixer in Satellite Cells. Breeding of *Mymx*$^{loxP1,2/+}$ and *Mymx*$^{loxP3,4/+}$ mice with mice carrying a tamoxifen-regulated satellite cell-specific Cre recombinase (*Pax7*^{CreERT2}) transgene (22) allowed for deletion of Myomixer in SCs upon tamoxifen treatment. In the experiments below, we named the *Pax7*^{CreERT2}/*Mymx*$^{loxP1,2/loxP1,2}$ and *Pax7*^{CreERT2}/*Mymx*$^{loxP3,4/loxP3,4}$ mice collectively as knockout (KO) mice due to the absence of any phenotypic differences between these mice. Tamoxifen-treated littermates of the same sex of *Pax7*^{CreERT2}, *Mymx*$^{loxP1,2/loxP1,2}$, or *Mymx*$^{loxP3,4/loxP3,4}$ mice were collectively referred to as control mice.

To induce genetic deletion of Myomixer in SCs, we injected *Myomixer* KO mice with tamoxifen every 2 d over a period of 10 d before injury of skeletal muscle by cardiotoxin (CTX) injection (Fig. 2*A*). We confirmed the DNA recombination specifically in tamoxifen-treated KO mice by PCR amplification of genomic DNA extracted from noninjured extensor digitorum longus (EDL) muscles (Fig. 2*B*). The relatively low intensity of DNA-recombination bands compared with that detected in cultured fibroblasts reflects the fact that SCs account for only ~5% of total myonuclei in intact muscle tissues (25). Our previous results showed that *Myomixer* expression peaked at day (d) 3 post-CTX injection in skeletal muscles (14). To confirm that *Myomixer* gene expression was abolished by Cre-mediated recombination, we examined *Myomixer* expression using a pair of quantitative PCR (qPCR) primers from the ORF region of exon 3, which was targeted in all lines of *Myomixer* KO mice. Of note, although gastrocnemius muscles from control mice showed a robust induction of *Myomixer* expression 3 d postinjury, this response was completely abolished in tamoxifen-treated KO mice (Fig. 2*C*). Myomixer protein was also not detectable in injured *Myomixer* KO gastrocnemius muscles, in contrast to control mice which expressed abundant Myomixer protein in injured gastrocnemius muscle (Fig. 2*D*).

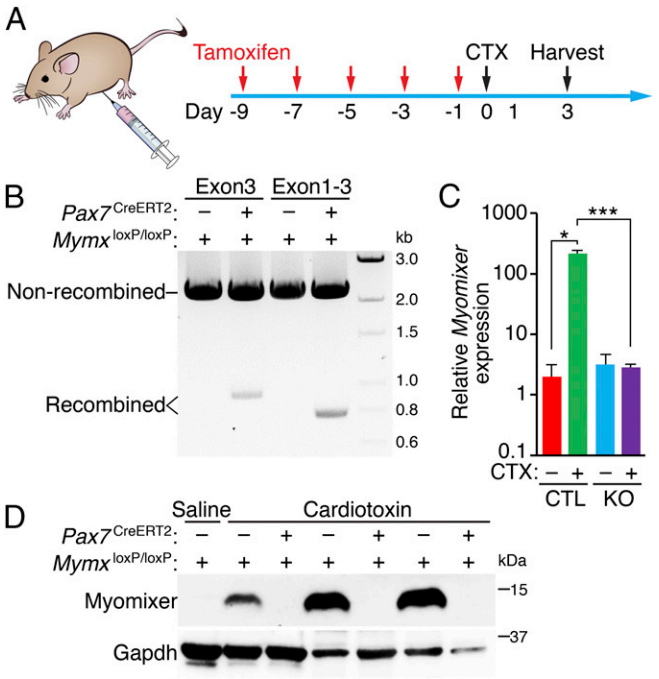

Fig. 2. Validation of Myomixer deletion in satellite cells. (*A*) Schematic outlining the strategy of tamoxifen and cardiotoxin treatment of mice. Control and *Myomixer* KO mice were treated with tamoxifen every 2 d over a period of 10 d before injury of skeletal muscle by cardiotoxin injection. Muscles were collected for analysis at 3 d postinjury. (*B*) PCR amplification of genomic DNA isolated from noninjured EDL muscles of *Mymx*$^{loxp1,2/1,2}$ (lane 1), *Pax7*^{CreERT2}/*Mymx*$^{loxp1,2/1,2}$ (lane 2), *Mymx*$^{loxp3,4/3,4}$ (lane 3), and *Pax7*^{CreERT2}/*Mymx*$^{loxp3,4/3,4}$ (lane 4) mice treated as shown in *A*. (*C*) Quantification by qPCR of *Myomixer* gene expression in gastrocnemius muscle 3 d postinjury. $n = 3$ for control (CTL) mice, $n = 5$ for *Myomixer* KO mice. (*D*) Western blot analysis of Myomixer and Gapdh in gastrocnemius muscle 3 d postinjury. $^{*}P < 0.05$; $^{***}P < 0.001$. Student's *t* test. Data are mean ± SEM.

Myomixer Is Not Required for Activation of the Myogenic Program in Satellite Cells. *Myomixer* KO mice following TMX-mediated gene deletion showed normal body weight, muscle mass, and myofiber architecture, based on hematoxylin and eosin (H&E) staining (Fig. S2). To evaluate the myogenic potential of SCs after genetic deletion of Myomixer, we analyzed expression of two key myogenic transcriptional regulators, Myod1 and Myogenin. These markers of SC activation were up-regulated 3 d postinjury in *Myomixer* KO mice, albeit to lower levels than in control mice (Fig. 3*A*).

We analyzed the consequences of loss of Myomixer in gastrocnemius muscles 3 d postinjury. H&E staining at this time point revealed abundant mononuclear cells, likely owing to inflammatory infiltration, myofibroblast proliferation, and SC activation (Fig. 3*B*). Muscles from control and *Myomixer* KO mice were nearly indistinguishable at 3 d postinjury, suggesting similar initial damage, immune response, and proper activation and differentiation of muscle precursors. We also examined the expression of terminal differentiation markers, Myogenin and Desmin, by immunohistochemistry. Cells positive for Myogenin and Desmin expression were clearly detected in injured *Myomixer* KO muscle (Fig. 3*C*). Additionally, as expected based on our previous results (21), *Myomaker* expression was robustly induced following muscle injury in control and *Myomixer* KO muscles (Fig. 3*A*). These results suggest that Myomixer is not required for activation of the myogenic program in SCs, consistent with our observations from deletion of Myomixer in cultured myoblasts and mouse embryos (14).

Myomixer Is Essential for Skeletal Muscle Regeneration. The peak of muscle regeneration typically occurs at 7 d postinjury (26), so we examined the muscle regenerative capacity at this time point (Fig. 4*A*). We measured the weights of injured and noninjured tibialis anterior (TA) muscles at this stage and used the ratio between the two measurements as the recovery ratio (Fig. S3). KO mice showed significant reductions of mass of injured TA muscle and recovery ratios compared with control mice, although the two genotypes showed similar mass measurements of noninjured TA muscles (Fig. S3). At the histological level, H&E staining of cross-sections of TA muscle revealed that control mice had a robust regenerative response, indicated by large myofibers containing centralized nuclei, a hallmark of muscle regeneration (Fig. 4*B*). In contrast, we observed a dramatic absence of regenerative myofibers in *Myomixer* KO mice (Fig. 4*B*). Instead, persistent infiltration of inflammatory cells was obvious in *Myomixer* KO muscles (Fig. 4*B*). Immunohistochemistry with antibodies against Myosin and Desmin on muscle at 7 d postinjury revealed a substantial loss of muscle cells in *Myomixer* KO muscle, suggesting that differentiated myoblasts die if they do not undergo fusion (Fig. 4*C*).

We also examined the regenerative response of *Myomixer* KO mice at 14 d postinjury, which marks the completion of muscle regeneration (Fig. 4 *D* and *E*). Although a nearly complete recovery of TA muscle mass was observed for control mice (97%), the mass of *Myomixer* KO-injured TA muscle was only 65% that

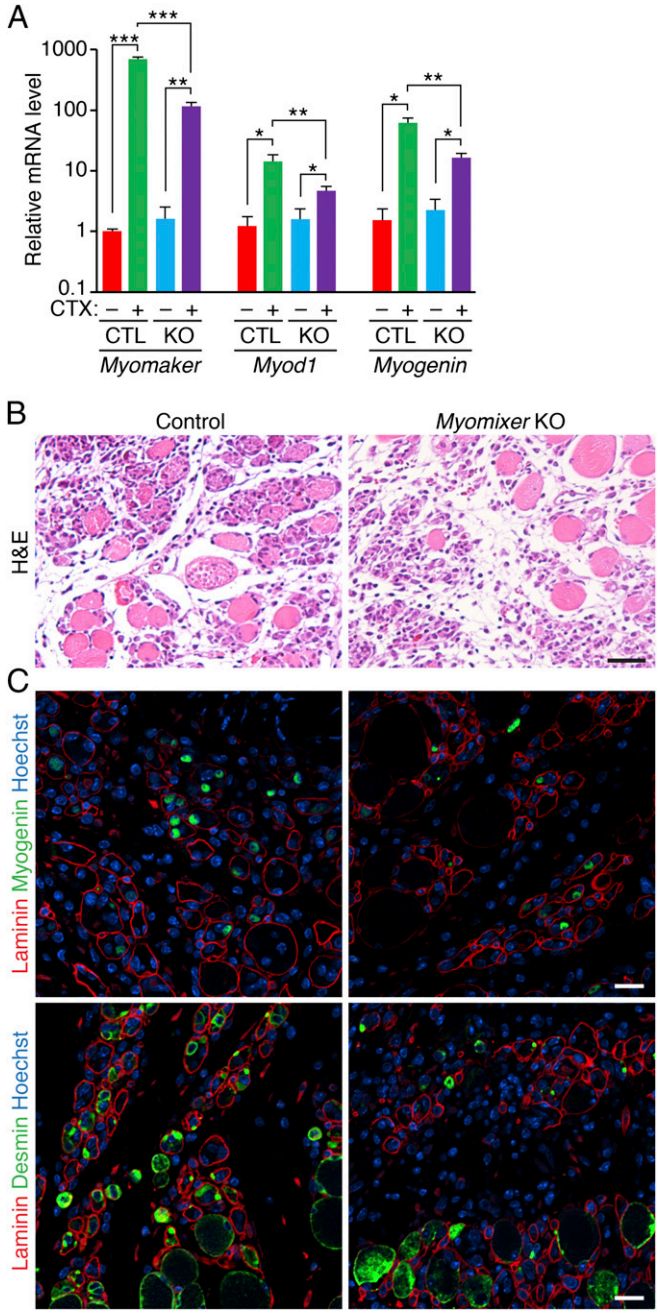

Fig. 3. Deletion of Myomixer in adult satellite cells does not affect the early response to muscle injury. (*A*) Quantification by qPCR of gene expression in gastrocnemius muscle 3 d postinjury. $n = 3$ for control (CTL) mice, $n = 5$ for *Myomixer* KO mice. (*B*) H&E staining of gastrocnemius muscle cross-sections at day 3 postinjury. (Scale bar: 50 μm.) (*C*) Immunohistochemistry of Laminin, Myogenin and Desmin in gastrocnemius muscle cross-sections at day 3 postinjury. (Scale bars: 20 μm.) $*P < 0.05$; $**P < 0.01$; $***P < 0.001$. Student's *t* test. Data are mean ± SEM.

of contralateral noninjured TA muscle (Fig. S3*B*). H&E staining of TA muscle cross-sections revealed that muscle architecture of control mice was fully recovered while *Myomixer* KO muscles showed regions of hypocellularity and small myofibers (Fig. 4*E*). Immunohistochemistry using antibodies against Myosin and Desmin on 14-d postinjury muscle confirmed the severe loss of regenerated myofibers containing centralized nuclei in *Myomixer* KO muscle (Fig. 4*F*). Together, these data demonstrate that Myomixer is essential for adult muscle regeneration.

Discussion

The results of this study show the requirement of Myomixer for skeletal muscle regeneration and underscore the obligate partnership of Myomixer and Myomaker, not only for myoblast fusion in developing muscle but also during adult skeletal muscle repair. Here we show by genetic deletion of Myomixer in adult SCs that Myomixer is absolutely essential for SC fusion in vivo, and its deletion results in a complete absence of regenerative myofibers following muscle injury. Of note, we did not observe any difference in the muscle regeneration response upon deletion of the short and long isoforms of Myomixer. This indicates that the weakly expressed long isoform, which contains an extra 24-amino acid extension at the N terminus, does not play an essential role in the fusogenic function of Myomixer. Accordingly, expression of the evolutionarily conserved short isoform in Myomixer KO myoblasts is sufficient to rescue the myoblast fusion defects as we previously reported (18). These findings parallel our previous study (21), which demonstrated that the lack of Myomaker abolishes adult muscle regeneration.

Intriguingly, we noticed that deletion of Myomixer in SCs decreased the abundance of Desmin$^+$ and Myogenin$^+$ muscle cells as well as the expression of muscle differentiation genes in regenerating muscles. These findings reinforce our previous observations in the developing muscles of Myomixer global knockout mouse, in which Myosin$^+$ cells appeared to be less abundant than those of wild-type mice (14). By contrast, in cultured myoblasts, deletion of Myomixer does not affect muscle differentiation gene expression (14). Therefore, we speculate that lack of fusion due to deletion of Myomixer affects myocyte viability, possibly due to feedback communications with nonmuscle cells at the peak of muscle development and regeneration.

Cell–cell fusion is involved in numerous biological processes in prokaryotic and eukaryotic cells (27, 28). In addition to skeletal muscle formation, cell fusion is required for fertilization of egg and sperm, as well as development of various organs (29). The placenta contains giant syncytiotrophoblasts that originate from fusion of mononuclear trophoblasts (30). Osteoclasts formed from fusion of mononuclear precursor cells are essential for the development and homeostasis of bone (31). Moreover, the generation of giant cells by fusion of macrophages is an integral part of the inflammatory response (29).

Cell fusion is a complex process that generally involves three fundamental steps: cell recognition and adhesion, merger of the proximal leaflets of membrane bilayers (known as hemifusion) and finally opening and expansion of a fusion pore that allows the exchange of cytosolic contents (28). Although these fundamental steps in membrane fusion are common, the molecular mechanisms that establish the cell-type specificity of these steps are not well understood.

The precise mechanism whereby Myomixer cooperates with Myomaker to drive myoblast fusion remains to be elucidated. Of note, structure–function analysis of Myomixer revealed key domains that are essential for its fusogenic function and conserved across multiple jawed vertebrates: an N-terminal hydrophobic domain, which is likely to function as a membrane anchoring region; a C-terminal hydrophobic AxLyCxL motif; and several charged residues in between that are required for binding Myomaker (14). A tentative model is that Myomaker works to position plasma membranes from two cells in close proximity to induce hemifusion, thereby allowing the hydrophobic AxLyCxL motif of Myomixer to function as a fusion peptide to establish the fusion pore, thus merging the plasma membranes. This working model closely mimics that of fusion-associated small transmembrane (FAST) proteins encoded by the nonenveloped fusogenic reoviruses (32). In this regard, insights into the mechanistic basis of FAST protein-induced fusion will be informative with respect to the mechanism of Myomaker–Myomixer-dependent fusion. In addition, studies to identify additional components

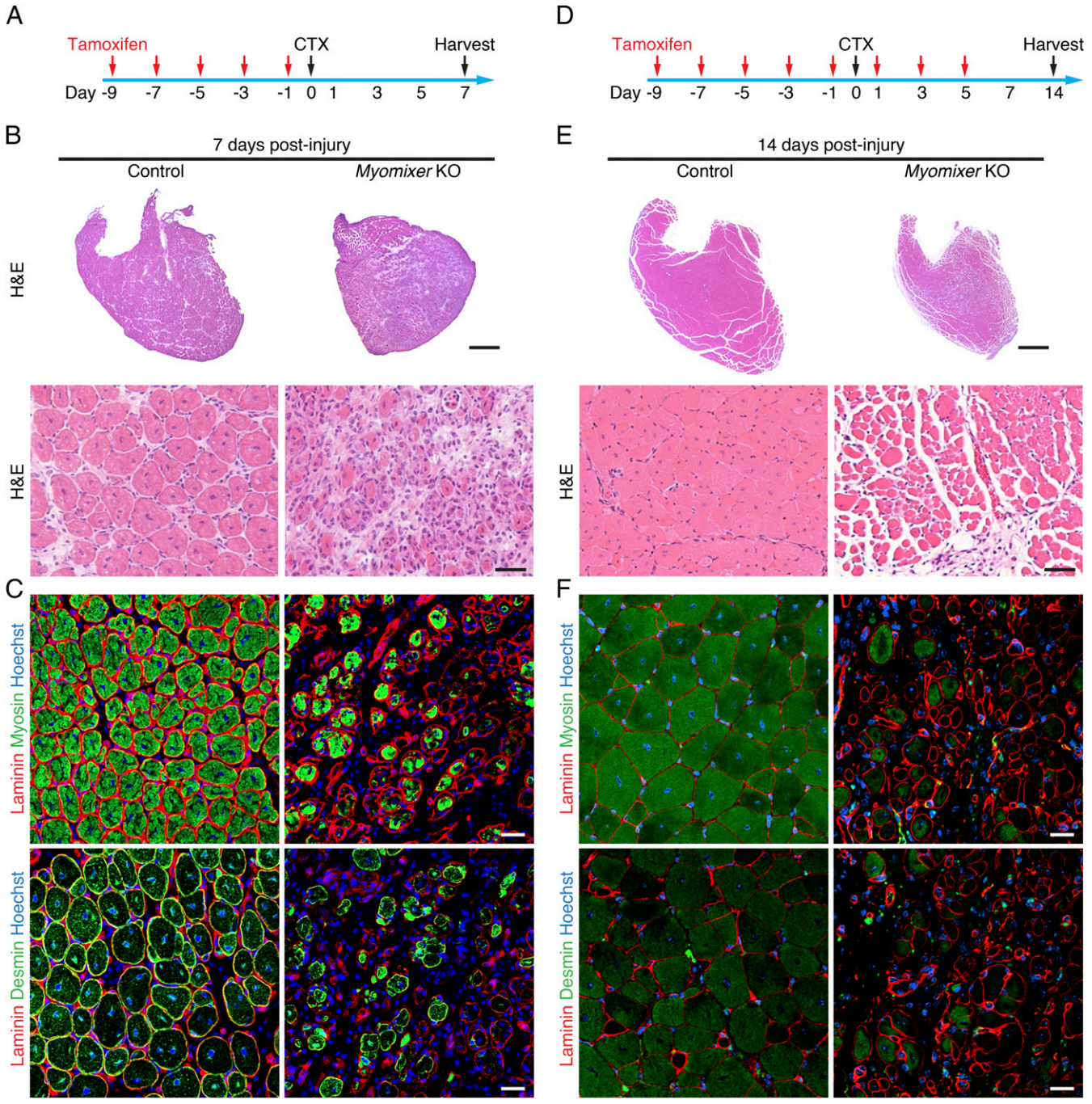

Fig. 4. Myomixer is essential for skeletal muscle regeneration after injury. (*A* and *D*) Schematic outlining strategy of tamoxifen and cardiotoxin treatment. (*B* and *E*) H&E staining of TA muscle cross-sections at (*B*) day 7 and (*E*) day 14 postinjury. (Scale bar: *Top*, 500 μm; *Bottom*, 50 μm.) (*C* and *F*) Immunohistochemistry of Laminin, Myosin, and Desmin on TA muscle cross-sections at (*C*) day 7 and (*F*) day 14 postinjury. (Scale bars: 20 μm.)

of the cellular fusion machinery that engage the Myomaker–Myomixer duo to drive membrane merger are underway.

Besides acute muscle regeneration, the Myomixer conditional alleles described here will be instrumental to investigate the full spectrum of Myomixer functionality, especially its potential role in long-term muscle homeostasis during aging, as well as muscle hypertrophy and disease conditions like cachexia and neuromuscular diseases. It will also be of interest to determine whether Myomixer is required in both SCs and myofibers during the hypertrophic response. The ability of Myomaker–Myomixer to promote fusion of nonmyogenic cells with each other or with preexisting muscle fibers also suggests opportunities for delivery of cellular cargo to target tissues in vivo through cell–cell fusion.

Materials and Methods

Generation of *Mymx*^{loxP} Mice. Animal work described in this manuscript was approved and conducted under the oversight of the University of Texas Southwestern Institutional Animal Care and Use Committee. Details of the generation of *Mymx*^{loxP} mice are provided in *SI Materials and Methods*.

Tamoxifen and Cardiotoxin Treatment. Details of the tamoxifen and cardiotoxin treatment of mice are provided in *SI Materials and Methods*.

Cell Cultures and Viral Infection. Primary myofibroblasts were isolated from 1-mo-old *Mymx*$^{loxP1,2/+}$ mice and *Mymx*$^{loxP3,4/+}$ mice. Briefly, skeletal muscle tissues were dissected and minced to a slurry with scissors followed by enzymatic digestion containing 1.5 units/mL collagenase D (11088858001, Sigma-Aldrich) and 2.4 units/mL dispase II (17105041, Thermo Fisher) in 2.5 mM $CaCl_2$. Fibroblasts were maintained in 10% FBS with 1% penicillin/streptomycin in DMEM. Upon confluency, the fibroblasts were split and infected with adenoviruses expressing GFP or Cre DNA recombinase for 2 d before being used for genomic DNA extraction and genotyping. Cre-mediated DNA recombination between the loxP sites was detected by PCR with a forward primer: 5′-GGGCTCCCTTGTGATGTCC-3′ and a reverse primer: 5′-TGCGTACACAAAAGTGCTCG-3′. This pair of primers is able to detect a 2,075-bp wild-type band, a 2,155-bp *Mymx*$^{loxP1/loxP2}$ or *Mymx*$^{loxP3/loxP4}$ band, a 924-bp recombination band upon deletion of a region containing exon 3, and a 777-bp recombination band upon deletion of a region containing exons 1–3. PCR genotyping products were gel purified and cloned into the pCRII Topo vector (K460001, Thermo Fisher) and sequenced to verify the genomic DNA recombination between loxP sites.

qPCR. Total RNA was extracted from mouse tissues with TRIzol (Invitrogen). cDNA was synthesized using iScript Reverse Transcription Supermix (1708841) using 1 μg RNA. Gene expression was assessed using standard qPCR approaches with KAPA SYBR FAST qPCR Master Mix (KK4605). Analysis was performed on a StepOnePlus Real-Time PCR System (Applied Biosystems) with the Sybr primers provided in *SI Materials and Methods*. The $2^{\Delta\Delta Ct}$ method was used to analyze the relative changes in gene expression normalized against *Gapdh* expression.

Western Blot Analysis. Protein was isolated from muscle tissues using RIPA buffer. Protein concentrations were determined using BCA Protein Assay Reagent (23225, Thermo Fisher Scientific) followed by measurement with NanoDrop. Protein samples were mixed with 4× Laemmli sample buffer (161–0747, Bio-Rad) and 20–40 μg protein was loaded and separated by Mini-PROTEAN TGX Precast Gels and transferred to a polyvinylidene fluoride (PVDF) membrane (Millipore), blocked in 5% fat-free milk for 1 h at room temperature, and then incubated with the following primary antibodies diluted in 5% milk overnight at 4 °C: Gapdh (MA5-15738, Thermo Fisher) and Myomixer (AF4580, R&D Systems). The HRP-conjugated secondary antibodies were as follows: donkey anti-sheep IgG-HRP (sc-2473, Santa Cruz Biotechnology) and goat anti-mouse IgG (H+L)-HRP conjugate (170–6516, Bio-Rad) were diluted at 1:5,000 in 5% milk. Immunodetection was performed using Western Blotting Luminol Reagent (sc2048, Santa Cruz Biotechnology).

H&E and Immunohistochemistry. For cryosections, skeletal muscle was dissected and embedded in tissue-freezing medium (TFM-5, General Data Healthcare) and frozen in 2-methylbutane cooled on dry ice. Transverse sections were cut at 10 μm and stained with H&E. For paraffin sections, skeletal muscles were fixed in 4% PFA/PBS for 24 h at room temperature, dehydrated, cleared, and wax infiltrated. Specimens were embedded transverse to myofiber long axis in Paraplast Plus (39602004, Leica) and sectioned at 5 μm to a depth containing regions of CTX injury or equivalent depths in contralateral control muscle. Resulting sections were deparaffinized, subjected to antigen retrieval, and immunostained with combinations of rabbit anti-laminin (L9393, 1:30; Sigma-Aldrich) and either mouse anti-myosin MY32 (M1570, 1:100; Sigma-Aldrich), mouse anti-myogenin F5D (SC52903, 1:50; Santa Cruz Biotechnology), or mouse anti-desmin DEU10 (D1033, 1:40; Sigma-Aldrich). Pronase E digestion was used to reveal antigenic epitopes for laminin/myosin, and pH 6.0 citra heat was used for laminin/desmin and laminin/myogenin, respectively. Mouse-on-mouse (BMK2202, Vector) blocking and detection reagents were used in conjunction with FITC-avidin-DCS (A2011, Vector) to localize myosin-, myogenin-, and desmin-tagged epitopes, and Cy3-conjugated goat anti-rabbit secondary antibody (111–165-144, Jackson Immunoresearch) to localize laminin. All preps were coverslipped with Vectashield and imaged on a Zeiss Meta 510C confocal microscope.

ACKNOWLEDGMENTS. We thank J. Cabrera for graphics, C. Perry and K. White (Histo Pathology Core, University of Texas Southwestern Medical Center) for technical assistance, Z. Wang and N. Liu for biological materials, and the other members of the E.N.O. laboratory for technical advice and discussion. This work was supported by grants from the NIH (AR-067294, HL-130253, and HD-087351) and the Robert A. Welch Foundation (Grant 1-0025 to E.N.O.).

1. Bentzinger CF, Wang YX, Rudnicki MA (2012) Building muscle: Molecular regulation of myogenesis. *Cold Spring Harb Perspect Biol* 4:a008342.
2. Liu N, et al. (2017) A Twist2-dependent progenitor cell contributes to adult skeletal muscle. *Nat Cell Biol* 19:202–213.
3. Lepper C, Partridge TA, Fan CM (2011) An absolute requirement for Pax7-positive satellite cells in acute injury-induced skeletal muscle regeneration. *Development* 138: 3639–3646.
4. Pawlikowski B, Pulliam C, Betta ND, Kardon G, Olwin BB (2015) Pervasive satellite cell contribution to uninjured adult muscle fibers. *Skelet Muscle* 5:42.
5. Brack AS, Rando TA (2012) Tissue-specific stem cells: Lessons from the skeletal muscle satellite cell. *Cell Stem Cell* 10:504–514.
6. Mauro A (1961) Satellite cell of skeletal muscle fibers. *J Biophys Biochem Cytol* 9: 493–495.
7. Le Grand F, Rudnicki MA (2007) Skeletal muscle satellite cells and adult myogenesis. *Curr Opin Cell Biol* 19:628–633.
8. Cheung TH, Rando TA (2013) Molecular regulation of stem cell quiescence. *Nat Rev Mol Cell Biol* 14:329–340.
9. von Maltzahn J, Jones AE, Parks RJ, Rudnicki MA (2013) Pax7 is critical for the normal function of satellite cells in adult skeletal muscle. *Proc Natl Acad Sci USA* 110: 16474–16479.
10. Abmayr SM, Pavlath GK (2012) Myoblast fusion: Lessons from flies and mice. *Development* 139:641–656.
11. Hindi SM, Tajrishi MM, Kumar A (2013) Signaling mechanisms in mammalian myoblast fusion. *Sci Signal* 6:re2.
12. Kim JH, Jin P, Duan R, Chen EH (2015) Mechanisms of myoblast fusion during muscle development. *Curr Opin Genet Dev* 32:162–170.
13. Millay DP, et al. (2013) Myomaker is a membrane activator of myoblast fusion and muscle formation. *Nature* 499:301–305.
14. Bi P, et al. (2017) Control of muscle formation by the fusogenic micropeptide myomixer. *Science* 356:323–327.
15. Millay DP, et al. (2016) Structure-function analysis of myomaker domains required for myoblast fusion. *Proc Natl Acad Sci USA* 113:2116–2121.
16. Quinn ME, et al. (2017) Myomerger induces fusion of non-fusogenic cells and is required for skeletal muscle development. *Nat Commun* 8:15665.
17. Zhang Q, et al. (2017) The microprotein Minion controls cell fusion and muscle formation. *Nat Commun* 8:15664.
18. Shi J, et al. (2017) Requirement of the fusogenic micropeptide myomixer for muscle formation in zebrafish. *Proc Natl Acad Sci USA* 114:11950–11955.
19. Zhang W, Roy S (2017) Myomaker is required for the fusion of fast-twitch myocytes in the zebrafish embryo. *Dev Biol* 423:24–33.
20. Landemaine A, Rescan PY, Gabillard JC (2014) Myomaker mediates fusion of fast myocytes in zebrafish embryos. *Biochem Biophys Res Commun* 451:480–484.
21. Millay DP, Sutherland LB, Bassel-Duby R, Olson EN (2014) Myomaker is essential for muscle regeneration. *Genes Dev* 28:1641–1646.
22. Lepper C, Conway SJ, Fan CM (2009) Adult satellite cells and embryonic muscle progenitors have distinct genetic requirements. *Nature* 460:627–631.
23. Trapnell C, et al. (2010) Transcript assembly and quantification by RNA-Seq reveals unannotated transcripts and isoform switching during cell differentiation. *Nat Biotechnol* 28:511–515.
24. Richardson CD, Ray GJ, DeWitt MA, Curie GL, Corn JE (2016) Enhancing homology-directed genome editing by catalytically active and inactive CRISPR-Cas9 using asymmetric donor DNA. *Nat Biotechnol* 34:339–344.
25. Snow MH (1981) Satellite cell distribution within the soleus muscle of the adult mouse. *Anat Rec* 201:463–469.
26. Liu N, et al. (2012) microRNA-206 promotes skeletal muscle regeneration and delays progression of Duchenne muscular dystrophy in mice. *J Clin Invest* 122:2054–2065.
27. Brizzio V, Gammie AE, Nijbroek G, Michaelis S, Rose MD (1996) Cell fusion during yeast mating requires high levels of a-factor mating pheromone. *J Cell Biol* 135: 1727–1739.
28. Podbilewicz B (2014) Virus and cell fusion mechanisms. *Annu Rev Cell Dev Biol* 30: 111–139.
29. Aguilar PS, et al. (2013) Genetic basis of cell-cell fusion mechanisms. *Trends Genet* 29: 427–437.
30. Lu X, et al. (2017) Fine-tuned and cell-cycle-restricted expression of fusogenic protein syncytin-2 maintains functional placental syncytia. *Cell Rep* 21:1150–1159.
31. Ishii M, Saeki Y (2008) Osteoclast cell fusion: Mechanisms and molecules. *Mod Rheumatol* 18:220–227.
32. Ciechonska M, Duncan R (2014) Reovirus FAST proteins: Virus-encoded cellular fusogens. *Trends Microbiol* 22:715–724.